

Miscibility, crystallization and melting behaviour and semicrystalline morphology of ternary blends of poly(ϵ -caprolacton), poly(hydroxy ether of bisphenol A) and poly(styrene-*co*-acrylonitrile): 2. Semicrystalline morphology

M. Vanneste, G. Groeninckx* and H. Reynaers

Katholieke Universiteit Leuven (KULeuven), Department of Chemistry, Laboratory for Macromolecular Structural Chemistry, Celestijnenlaan 200F, B-3001 Heverlee, Belgium
 (Revised 14 November 1996)

The semicrystalline morphology of pure PCL and of some of its *miscible* binary and ternary blends with Phenoxy and SAN15 has been investigated by small angle X-ray scattering. Morphological parameters have been obtained from the analysis of the one-dimensional correlation function. The influence of the crystallization temperature on the semicrystalline morphology has been investigated and is compared with the melting behaviour as studied with differential scanning calorimetry. © 1997 Elsevier Science Ltd.

(Keywords: semicrystalline morphology; SAXS; segregation behaviour)

INTRODUCTION

Small angle X-ray scattering (SAXS) has proved to be a powerful tool in the investigation of the semicrystalline morphology of polymers. Although considerable experience has been gained in analysing SAXS patterns of semicrystalline homopolymers^{1–5}, the field of semicrystalline polymer blends appears to be less documented^{6–13}. The morphology of poly(ϵ -caprolacton) (PCL) and some of its binary blends with poly(vinyl chloride) (PVC)^{14–16}, polycarbonate (PC)¹⁷, poly(styrene-*co*-acrylonitrile) (SAN)^{17,18}, poly(styrene-*co*-maleicohydride) (SMA)¹⁹, Phenoxy²⁰ and polystyrene (PS)²¹ has been investigated in the past. To our best knowledge, only the ternary PCL/SAN15/SMA14 blend studied in our laboratory was investigated with SAXS²².

Crystallization in a polymer blend involves two types of polymer transport: diffusion of the crystallizable component towards the crystal growth front and a simultaneous rejection of the amorphous component(s). The latter phenomenon is called segregation. Segregation can take place on three different levels, interspherulitic, interfibrillar and interlamellar. Interspherulitic segregation, in which the spherulites are imbedded in an amorphous matrix, can be distinguished from the other two types by optical microscopy. In the case of intraspherulitic segregation, a volume-filling texture is observed. SAXS is a useful technique to find out whether or not interlamellar segregation occurs. An increase of the long spacing (or the amorphous layer thickness) in the blend with increasing concentration of the amorphous

component has been considered in the past to be decisive proof for interlamellar segregation. The average long spacing, $\langle L \rangle$, is defined as the sum of the average thicknesses of the crystalline and the amorphous layers, $L = \langle L_c \rangle + \langle L_a \rangle$.

The purpose of this paper is to study the semicrystalline morphology of the ternary polymer blend PCL/Phenoxy/SAN15 and to relate the morphological data with the melting and crystallization characteristics as reported in part 1 of this paper²³. It should be noted that *only the miscible* blends were studied (e.g. with 90 wt% PCL), as well as pure PCL.

EXPERIMENTAL

Poly(ϵ -caprolacton) (PCL), poly(hydroxy ether of bisphenol A) (Phenoxy) and poly(styrene-*co*-acrylonitrile) with 15 wt% acrylonitrile (SAN15) were blended by means of the dissolution-coprecipitation method; a 3% (w/v) THF solution was prepared, which was added subsequently to an excess of hexane as non-solvent. The blends obtained were dried *in vacuo* during 3 days at 45°C. Phenoxy was obtained from Aldrich; PCL was kindly supplied by Solvay (Capsa 630), and the SAN15 copolymer by DOW Terneuzen, Benelux, The Netherlands. The molecular characteristics of these polymers are presented in *Table 1*.

SAXS measurements were performed on a Rigaku rotating anode, operating at 7.5 kW, which was provided with a Kratky camera in the infinite slit geometry. Ni-filtered Cu-K α radiation was used throughout and the sample irradiation time was 1 h. The SAXS data were collected using a one-dimensional position sensitive

* To whom correspondence should be addressed

Table 1 Molecular characteristics of the polymers used in this study

Blend components	M_w	M_n	M_w/M_n	T_g (°C)	T_m (°C)
PCL	57 000	38 000	1.49	-55	60
Phenoxy	45 000	18 000	2.59	91	/
SAN15	149 000	71 000	2.11	113	/

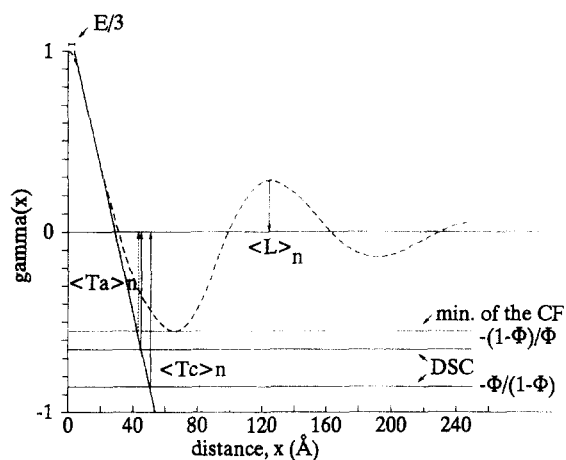


Figure 1 Schematic presentation of a one-dimensional correlation function ($\gamma(x)$ versus x) and the morphological parameters that can be derived from it (L , long spacing; $\langle T_c \rangle_n$ and $\langle T_a \rangle_n$, number average thickness of the crystalline and amorphous layer, respectively; E , width of the transition layer; ϕ , crystallinity)

proportional counter (McBraun GmbH). The SAXS data were subsequently converted to ASCII files and data treatment was done by the program FFSAXS²⁴. A detailed description about the experimental route and the data treatment has been given elsewhere²⁵. The original data were smoothed, background corrected and desmeared. These results led to several correlations between the scattered intensity and the scattering vectors (e.g. original smeared intensity curve, desmeared scattering curve, Lorentz corrected intensity function, three and one-dimensional correlation functions). The most important morphological parameters were derived from the desmeared Lorentz corrected intensity functions and from the analysis of the one-dimensional correlation functions.

The periodicity present within the stacks of lamellae constituting the spherulitic morphology can be indicated by means of the long spacing L , which is defined as the average distance including an amorphous and a crystalline layer. The number average long spacing $\langle L \rangle_n$ can be obtained from the correlation function approach ($\gamma(x)$ vs x , Figure 1).

The lamellar morphology of polymers has been described by an ideal two-phase model of alternating crystalline and amorphous layers involving an infinite gradient in electron density. Accumulating experimental evidence, however, made clear that most semicrystalline polymers and blends do not fit into this model, since the presence of a transition layer between the phases cannot be neglected. Other models²⁶ have been developed using different kinds of electron density profiles.

The presence of a transition layer can be observed and predicted from the correlation function because a curvature at the origin of the $\gamma(x)$ vs x plot is observed. The construction of a straight line tangent to the 'self-correlation triangle' (or to the initial linear region of the

correlation function) permits estimation of $E/3$ (E = the width of the transition layer), being the x -value corresponding to the intersection of the straight line and the y -value that equals identity ($y = 1$, see Figure 1).

The shape of the experimental correlation function by itself informs on the morphology of the underlying superstructure: curvature of the function at the origin points to the presence of a transition layer, while the absence of a plateau in the first minimum indicates a degree of crystallinity by volume somewhere between 35 and 65%. This inherent weakness of the correlation function approach can be overcome if crystallinity values determined by means of another technique, e.g. wide angle X-ray scattering, differential scanning calorimetry (d.s.c.), density measurements, are available^{27,28}. The errors involved in the determination of the average thickness of the crystalline ($\langle T_c \rangle_n$) and the amorphous layers ($\langle T_a \rangle_n$) with the method as presented in Figure 1 are not equal for both parameters. This is obvious since the slope of the self-correlation triangle is extrapolated to the straight line corresponding to $-(1-\phi)/\phi$ and to $-\phi/(1-\phi)$, respectively. Variation of the position of the straight line tangent to the correlation function results in a larger difference in the value of $\langle T_c \rangle_n$. From Figure 1 it is also clear that the use of the crystallinity determined from the minimum of the correlation in the absence of a clear plateau (dotted lines) leads to incorrect values of the morphological parameters.

For the thermal treatment of the samples during irradiation, an in-house made heating device was used with a precision of 0.1°C. D.s.c. scans (DSC7 Delta Series of Perkin Elmer) were performed under analogous conditions as used in the X-ray measurements in order to be able to relate the melting behaviour with the morphology. The same heating pretreatment was given to the samples in both techniques.

ANALYSIS OF THE SCATTERING DATA

In this part (part 2) only the miscible ternary blends will be investigated (e.g. with 90 wt% PCL), as well as pure PCL.

Adding 10 wt% amorphous material to PCL or varying the blend composition (ratio SAN to the total amount of amorphous material) results in a very slight, although a systematic increase of the long spacing, a tendency which is more pronounced the higher the amount of SAN15 in the blend (Figure 2).

Adding 10 wt% amorphous material to PCL results in a decrease of the core thickness, $C (= \langle T_c \rangle_n - E)$ for all blends as compared to the core thickness of pure PCL (Figure 3). The mentioned parameters are outlined in Figure 4. For all blends C increases with increasing concentration of SAN15 (or decreasing amount of Phenoxy).

The variation of the average thickness of the amorphous layer, $A (= \langle T_a \rangle_n - E)$ seems to depend

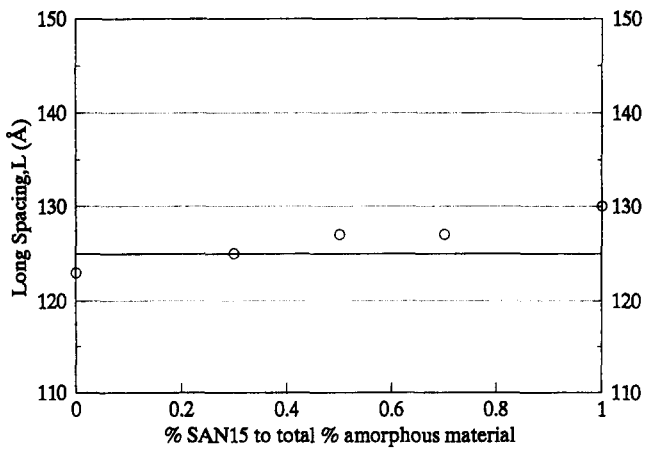


Figure 2 Number-average long spacing ($\langle L \rangle_n$) determined by the correlation function approach (solid line, pure PCL; symbols, blends)

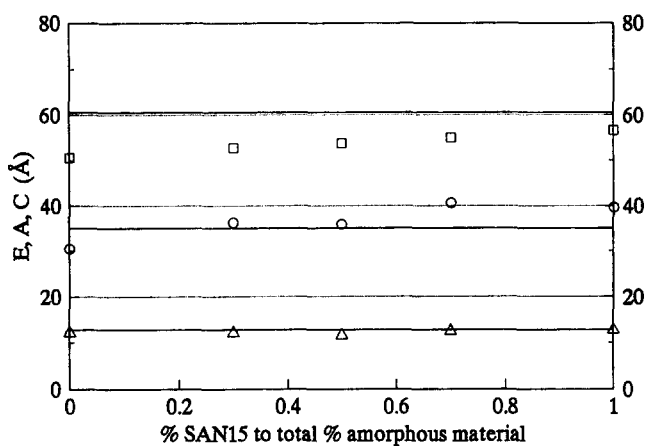


Figure 3 Morphological parameters derived from the correlation function: C and A , thickness of the crystalline core, and of the amorphous layer, respectively; E , width of the transition layer (C , squares; A , circles; E , triangles; solid lines, pure PCL; symbols, blends)

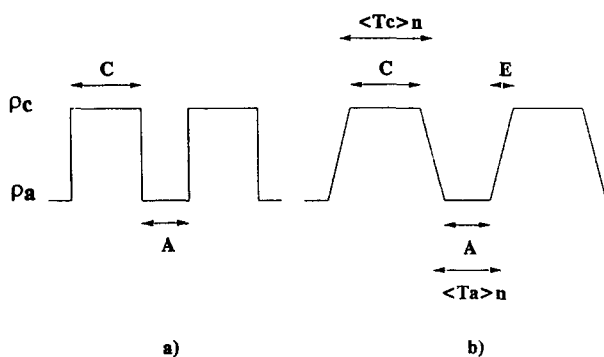


Figure 4 Model of alternating crystalline and amorphous layers with (a) a sharp boundary (ideal two phase model); (b) a diffuse transition layer inbetween (pseudo two-phase model) ($C = \langle T_c \rangle_n - E$, crystalline core; $A = \langle T_a \rangle_n - E$, amorphous layer thickness; E , transition layer; ρ_c and ρ_a , the electron density of the crystalline and amorphous phase, respectively)

more on the type and the amount of amorphous material that is added (Figure 3) than the semicrystalline core thickness does. The binary PCL/Phenoxy blend exhibits a smaller value for A than pure PCL. A gradual increase of the amorphous layer thickness is noticed with increasing SAN15 concentration which finally results in a higher value of A as compared to pure PCL.

The value of A is very important with respect to the understanding of the segregation behaviour of the amorphous polymers (Phenoxy and SAN15) in a semicrystalline blend. In Figure 5 the three types of segregation are schematically presented. As already mentioned in the Introduction, interlamellar segregation can be detected with SAXS from an increase of the amorphous layer thickness. This tendency is actually observed on adding SAN15 to PCL, suggesting that SAN15 is segregated interlamellarly and Phenoxy interfibrillarly since no increase of A is noticed in the binary PCL/Phenoxy blend. The ternary blends exhibit an intermediate behaviour depending upon the ratio of Phenoxy to SAN15 in the blend. These results are consistent with other studies performed on PCL/SAN blends¹⁷. SAXS studies performed on the binary PCL/SAN24¹⁸ and PCL/Phenoxy²⁰ blends resulted in an interlamellar segregation and in a interlamellar or interfibrillar segregation depending on the blend composition, respectively. However, the type of segregation of the amorphous components in the latter cases (PCL/SAN24 and PCL/Phenoxy) was solely based on the observation of the variation of the long spacings as a function of blend composition.

A surprising observation is the decrease of the amorphous layer thickness in the binary PCL/Phenoxy blend as compared to pure PCL. The good miscibility of PCL and Phenoxy (by strong interactions due to hydrogen bonding) may be responsible for the fact that in the PCL/Phenoxy blends PCL is located to a larger extent between stacks of lamellae than in the pure homopolymer where the amorphous fraction of PCL is present in the interlamellar zones.

In Figure 6 the correlation functions of PCL/Phenoxy/SAN15 90/00/10, crystallized at different temperatures, are shown. From the shape of the curves the following conclusions can be derived: the first minimum shifts to higher values with increasing crystallization temperature (T_c) indicating a change in crystallinity and the first maximum shifts to higher x -values corresponding to a larger long spacing. The morphological parameters calculated conform to the procedure of Figure 1, and are presented in Figure 7.

A first observation is the slight increase of the width of the transition layer (E) which can be attributed to thermal expansion. Secondly, the thickness of the amorphous layers (A) increases drastically, probably due to the melting of the thinnest lamellae and at high temperatures even of the spherulites. Finally, an increase of the crystalline layer thickness (C) is observed for relatively low T_c , while a decrease is noticed at higher T_c .

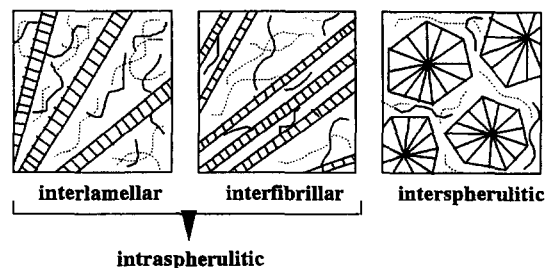


Figure 5 Schematic presentation of the different types of segregation of the amorphous component(s) in crystallizable polymer blends (full lines, crystallizable component; dotted lines, amorphous component)

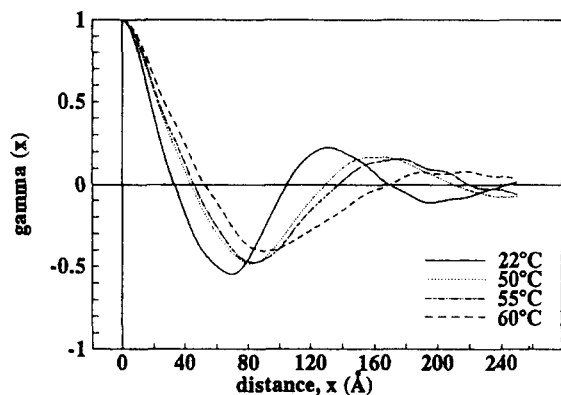


Figure 6 Correlation functions of the PCL/Phenoxy/SAN15 90/00/10 blend reflecting the influence of the crystallization temperature on the semicrystalline morphology

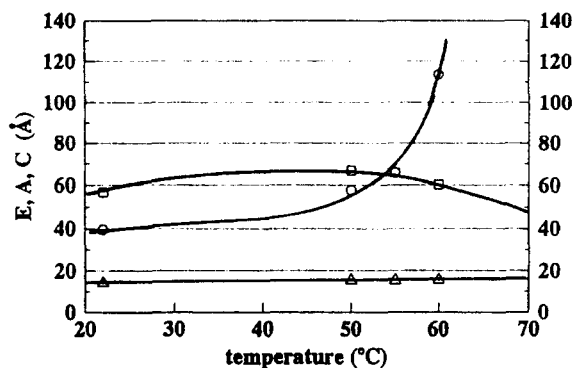


Figure 7 Influence of the crystallization temperature on the morphological parameters of the PCL/Phenoxy/SAN15 90/00/10 blend (C and A , thickness of the crystalline core, and of the amorphous layer, respectively; E , width of the transition layer; C , squares; A , circles; E , triangles)

(55 and 60°C). An explanation for these observations can be found when the corresponding d.s.c. thermograms are investigated (Figure 8). The same temperature pretreatment (Figure 9) was applied to all the samples as for the SAXS measurements. PCL and its binary and ternary blends with Phenoxy and SAN15 exhibit a complex melting behaviour as evidenced by the presence of two melting endotherms²³. Increasing the crystallization temperature results in a shift of both melting endotherms to higher temperatures (explaining the initial increases of C) which is however more pronounced for the lower melting peak. In the SAXS study the temperature was increased from 22 to 60°C, corresponding to a shift of both melting peaks to higher temperatures in the d.s.c. thermograms (Figure 8); however there is a concomitant decrease in crystallinity on going from 22 to 60°C. These observations indicate that at those temperatures the spherulites are already melting, as confirmed by the decrease of the crystalline core thickness, C , and a considerable increase of the amorphous layer thickness, A (Figure 7), while the d.s.c. melting endotherms (Figure 8) become broader and smaller (in height).

CONCLUSIONS

SAXS was used to highlight some aspects of the semicrystalline morphology of pure PCL and the PCL/Phenoxy/SAN15 blends with 90 wt% PCL. The level of

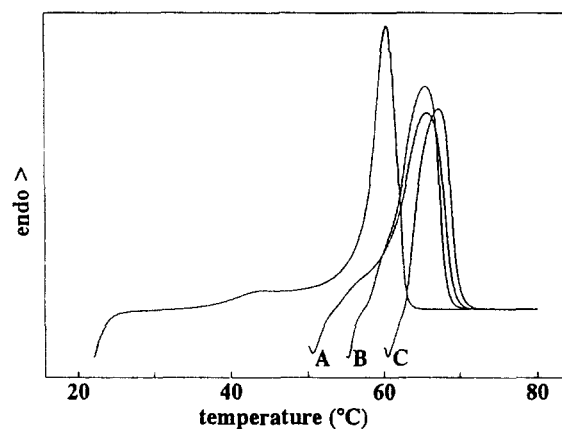


Figure 8 D.s.c. thermograms of the PCL/Phenoxy/SAN15 90/00/10 blend simulating the SAXS measurements presented in Figure 7 (symbols A, B and C refer to the temperature treatment used and presented in Figure 9)

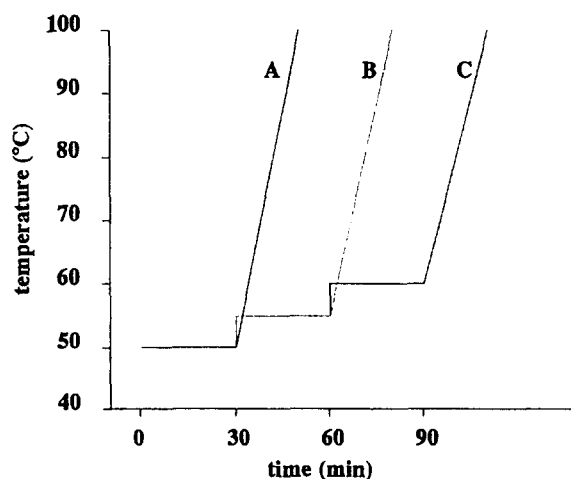


Figure 9 Schematic presentation of the temperature (pre) treatment of the d.s.c. samples

segregation of Phenoxy and SAN15 was determined by calculation of the long spacing (L), the crystalline core thickness (C), the thickness of the amorphous layers (A) and the width of the transition layer (E). While SAN15 is segregated interlamellarly, Phenoxy is located in the interfibrillar zones. The ternary blends exhibit an intermediate behaviour depending upon the blend composition. The influence of the temperature on the morphological parameters (L , C , A and E) reveals a considerable increase of the amorphous layer thickness and a concomitant decrease in the crystalline core thickness with increasing crystallization temperature.

ACKNOWLEDGEMENTS

The authors are indebted to the I.W.N.O.L. for the grant offered to M.V. and to the Belgian National Science Foundation (N.F.W.O.) for financial support given to the MSC laboratory.

REFERENCES

- Schouterden, P., Vandermarliere, M., Riekkel, C., Koch, M. H. J., Groeninckx, G. and Reynaers, H., *Macromolecules*, 1989, **22**, 237.
- Defoor, F., Groeninckx, G., Reynaers, H., Schouterden, P. and Van der Heijden, B., *Macromolecules*, 1993, **26**, 2575.

3. Barham, P. J. and Keller, A., *J. Polym. Sci., Polym. Phys. Edn.*, 1989, **27**, 1029.
4. Strobl, G. and Schneider, M., *J. Polym. Sci., Polym. Phys. Edn.*, 1980, **18**, 1343.
5. Vonk, C. G., *J. Appl. Cryst.*, 1973, **6**, 81.
6. Wenig, W., Karasz, F. E. and MacKnight, W. J., *J. Appl. Phys.*, 1975, **46**, 4194.
7. Warner, F. P., MacKnight, W. H. and Stein, R. S., *J. Polym. Sci. Polym. Phys. Edn.* 1977, **15**, 2113.
8. Wasiak, A. and Wenig, W., *Colloid Polym. Sci.*, 1984, **262**, 435.
9. Wenig, W. and Schöller, T., *Angew. Makromol. Chem.*, 1985, **130**, 155.
10. Wenig, W. and Schöller, T., *Prog. Colloid Polym. Sci.*, 1985, **71**, 113.
11. Fiedel, H. W., Schöller, T., Petermann, J. and Wenig, W., *Colloid Polym. Sci.*, 1986, **264**, 1017.
12. Fiedel, H. W. and Wenig, W., *Colloid Polym. Sci.*, 1989, **269**, 389.
13. Silvestre, C., Karasz, F. E., MacKnight, W. J. and Martuscelli, E., *Eur. Polym. J.*, 1987, **23**, 745.
14. Warner, F. P., MacKnight, W. J. and Stein, R. S., *J. Polym. Sci., Polym. Phys. Edn.*, 1977, **15**, 2113.
15. Russell, T. P. and Stein, R. S., *J. Macromol. Sci.*, 1980, **B17**, 617.
16. Nojima, S., Tsutsui, H., Urushihara, M., Kosaka, W., Kato, N. and Ashida, T., *Polym. J.*, 1986, **18**, 451.
17. Vandermarliere, M., Miscibility and morphology of polymer blends. Ph.D. dissertation, KULeuven, 1986.
18. Defieuw, G., Miscibility and semicrystalline morphology of binary and ternary blends of amorphous and crystalline polymers. Ph.D. dissertation, KULeuven. 1989.
19. Defieuw, G., Groeninckx, G. and Reynaers, H., *Polymer*, 1989, **30**, 2158.
20. Defieuw, G., Groeninckx, G. and Reynaers, H., *Polymer*, 1989, **30**, 2164.
21. Li, Y. and Jungnickel, B.-J., *Polymer*, 1993, **34**, 9.
22. Vanneste, M. and Groeninckx, G., *Polymer*, 1995, **36**, 4253.
23. Vanneste, M. and Groeninckx, G., *Polymer*, 1994, **34**, 1051.
24. Vonk, C. G., *J. Appl. Cryst.*, 1975, **8**, 340.
25. Vanneste, M., Ternary polymer blends, miscibility, crystallization and melting behaviour, and semi-crystalline morphology. Ph.D. dissertation, KULeuven, 1994.
26. Balta-Calleja, F. J. and Vonk, C. G., in *X-Ray Scattering of Synthetic Polymers*, Polymer Science Library, 8, ed. A. D. Jenkins. Elsevier Science.
27. Mandelkern, L., *Crystallization of Polymers*. McGraw-Hill, New York, 1963, p. 305.
28. Mandelkern, L., *Acts Chem. Res.*, 1990, **23**, 380.